International Journal Of
Industrial Electronics Control and Optimization
Print ISSN: 3517-2645
Online ISSN: 3568-2645
Homepage: https://ieco.usb.ac.ir/

High Impedance Fault Detection in Power Transmission Lines Using Hilbert Transform and Instantaneous Frequency

Hassan Abniki[1, 2] | Mostafa Hajati Samsi[3] | Behrooz Taheri[4] | Seyed Amir Hosseini[5]

Deputy Director General of the Office of Research and Technology Development, Tavanir Co., Tehran, Iran.[1]
ECE School, University of Tehran, Tehran, Iran.[2]
Department of Electrical Engineering, Vebko Amirkabir research and development Co., Tehran, Iran.[3]
Department of Electrical Engineering, Qazvin Branch, Islamic Azad University, Qazvin, Iran.[4]
Electrical and Computer Engineering Group, Golpayegan College of Engineering, Isfahan University of Technology, Golpayegan, Iran.[5]
Corresponding author's email: s.hosseini@iut.ac.ir

Article Info

Article type:
Research Article

Article history:
Received: 2022 July 06
Received in revised form: 2022 Nov 26
Accepted: 2022 Dec 05
Published online: 2023 Jan 22

Keywords:
High Impedance Fault,
Power System Protection,
Power Transmission Lines,
Hilbert Transform.

ABSTRACT

Power transmission lines are vital components of today's power systems. These power lines transmit the electricity produced in power plants in high volume and with very low losses to distant areas so that it can be reached consumers through distribution networks. In fact, these lines are the intermediary between major energy producers and distribution networks. Accordingly, these transmission lines are of great importance and must be protected appropriately with a suitable protection system. Distance relays are widely used to protect these lines due to their convenient coordination characteristics and simplicity. High impedance faults (HIFs) can be a critical challenge for distance relays due to their low current amplitude and similarity to conventional events in power systems, such as capacitive bank switching. Therefore, this paper presents a new approach based on the instantaneous frequency variations obtained from the current RMS to detect HIFs. This method detects HIFs by calculating a detection index (DI) and considering a threshold value. The proposed method was tested using DIgSILENT and MATLAB software in an IEEE standard 39-bus network. The presented results evidently demonstrate that the proposed method is suitable for detecting HIF and low impedance faults (LIFs). In addition, this method has a proper performance during capacitor bank switching and can well distinguish between HIFs and capacitive bank switching. Moreover, the presented method is resistant to noise and is also capable of detecting the faulty phase.

I. Introduction

A. Motivation

Due to random nature and environmental conditions, the probability of fault that occurs is very high in power systems [1]. Therefore, power systems require a proper protection system. An ideal protection system that can operate accurately and timely can reduce damage to network equipment and even humans [2]. Among the various protection designs and relays, distance relays are an integral part of power system protection. Some desirable features of distance relays include simplicity, use of local voltage and current for fault detection, and fault locating capability [3]. Such characteristics have made distance relays a very beneficial means for power transmission line protection. Nevertheless, despite their numerous advantages, these relays also suffer from some shortcomings. One of the problems associated with distance relay algorithms is malfunctioning during high impedance faults (HIFs). Low current values and electric arcs distort the current during HIF. Besides, the current is very asymmetric and unstable during

HIF. In addition, the transient states of this type of fault are very similar to load switching and capacitive bank switching [4]. Failure to detect HIFs promptly may cause severe damage to network equipment and humans [5, 6].

B. Literature review

Despite the importance of HIF detection in power transmission lines, most research in this field has focused on distribution systems in recent years. Although the main purpose of this paper is to detect HIFs on power transmission lines, HIF detection methods in distribution networks have also been explored to have a more thorough evaluation.

Reference [1] employs discrete wavelet transform (DWT) and root mean square (RMS) values to identify and classify HIFs. Methods that use DWT require a high sampling rate for detection. In addition, this reference does not implement its method during signal noise [7]. In reference [8], the time-domain of current waveforms is only analyzed using the Kullback-Leibler divergence similarity measure. Authors in this reference use a time-based criterion to correctly identify HIFs. Reference [9] uses time domain analysis to detect HIF. Reference [10] uses a transient switching method to detect HIFs. Although the performance of this method is suitable, it cannot detect the faulty phase. References [11, 12] use a combination of DWT, fuzzy logic, and artificial neural networks (ANN) to detect HIFs. Although intelligent methods are accurate, they must be trained with a variety of simulations. In addition, these methods may be sensitive to noise. Reference [13] presents an HIF detection scheme based on empirical mode decomposition (EMD) in a DC microgrid. Reference [14] presents a method based on changes in active and reactive power components for HIF detection in DC microgrids.

This method may also respond differently in different networks. Reference [15] presents a method based on measuring the current at both ends of the transmission line and using differential protection. The main shortcoming of this method is its dependency on telecommunication platforms. Implementing telecommunication links will increase the fault detection time due to inheritance delay. Reference [16] uses correlation functions for fault detection. Mathematical morphology is used to identify HIFs in references [17, 18]. To implement such methods, relays suffer from heavy calculations. Reference [19] uses traveling waves to locate HIF. These methods require special equipment that increases the cost of implementing the protection system. In addition, in some studies on power swing detection, such as references [20-22], the ability to detect HIF has been investigated as a case. In these studies, an appropriate HIF model is not implemented. In addition, these studies can only detect faults with impedances below 150 ohms. Studies on HIF diagnosis can be categorized from different perspectives, including method, sampling rate, sampling method, solution method, and so on. Table (1) presents some recent studies on HIF diagnosis and their differences from the present article.

C. Contributions and organization

As mentioned, HIF detection in power systems is an issue of great importance. Besides, speed and accuracy in HIF detection are also crucial. Reference [27] uses instantaneous frequency to detect power swings. This algorithm can detect a variety of faults in power systems with appropriate speed and accuracy at a sampling rate of 10 kHz. Although this article considers HIF as a case and HIF in the power system may have an impedance of more than 1000 [28], the approach presented in this paper cannot detect HIFs with values greater than 100 ohms. In addition, as the transmission lines get longer, this method may face some challenges to detect HIFs that have occurred at a very long distance from the relay. The main objective of this article is to modify the algorithm presented in reference [27] to improve its performance in the event of an HIF. Besides being resistant to noise and not malfunctioning during capacitive bank and load switching, the proposed new algorithm still enjoys a good fault detection speed. The modified algorithm can also detect the faulty phase.

This article is organized as follows. Section II formulates the problem. The simulation results are presented in Section II. Section IV compares the proposed method with similar research. Finally, the conclusion is presented in Section V.

II. Proposed method

To modify the algorithm presented in reference [27], the method of obtaining instantaneous frequency using the Hilbert transform should be investigated. For this purpose, this section describes the required relationships and the modified algorithm.

A. Hilbert Transform and instantaneous frequency

One of the most critical data in monitoring, protecting, and controlling power systems is frequency. Calculating the exact value of frequency for programs that are dependent on a quick response is an issue of great importance [29]. The conventional definition for instantaneous frequency (IF) is that IF is typically associated with the rate of change in phase angle. In this paper, IF is obtained using the Hilbert transform. Hilbert's transformation was first proposed by David Hilbert to characterize integral equations in physics and mathematics [30]. The Hilbert transform can be defined for a function as (1) [31-33].

$$H[X(t)] = \tilde{x}(t) = \pi^{-1} \int_{-\infty}^{+\infty} \frac{x(\tau)}{t-\tau} d\tau \quad (1)$$

The Hilbert transform is a mathematical transformation function that shifts the phase of a signal by 90 degrees without changing the amplitude of the signal. In fact, in the Hilbert transformation, the phase of positive frequency components is shifted by $+\ \pi/2$ and the phase of negative frequency components is shifted by $-\ \pi/2$. The Hilbert transform is an odd function and an even function.

TABLE I
RECENT STUDIES ON HIF DIAGNOSIS

Ref.	Year	Method	Voltage	Detection / location	Requirement for a telecommunication link	Dependence on network parameters	Consideration of noise	Consideration of load switching	Consideration of capacitor bank switching	Faulty phase detection
[2]	2021	Impedance-based	HV	location	✓	✓	✓	×	×	✓
[23]	2021	Robust faulted phase	UHV	Detection	×	×	×	×	×	×
[24]	2021	Power spectral density	LV	Detection	×	×	✓	✓	✓	×
[25]	2020	Wavelet Transform	HV	Detection	×	×	×	×	×	×
[26]	2020	Wavelet transform	LV	Detection	×	×	✓	✓	✓	×
This paper	-	instantaneous frequency	HV	Detection	×	×	✓	✓	✓	✓

For the Hilbert transform, it is enough to obtain the Fourier transform of the function and multiply it with the $j.\text{sgn}(f)$ function in the Fourier domain. Subsequently, the inverse Fourier transform of the function is calculated. The resulting function is the Hilbert transform. $j.\text{sgn}(f)$ is the transfer function in the Hilbert transform (in (2)).

$$H(jw) = -j.\text{sgn}(w) \tag{2}$$

$$\text{sgn}(w) = \begin{cases} 1 & \text{w}>0 \\ 0 & \text{w}=0 \\ -1 & \text{w}<0 \end{cases} \tag{3}$$

The Hilbert transform is a linear operator, which consists of an input signal $f(r)$ and an output signal $f_1(r)$. If the frequency spectrum of an input and output signal were $f(w)$ and $f_1(w)$, respectively, the relationship between the frequency spectrum of the input and output signals would be similar to (4).

$$\begin{cases} F_1(w) = H(jw).F(w) \\ F_1(w) = -jF(w) \ \text{ for } \ \text{w} \geq 0, \\ F_1(w) = -jF(w) \ \text{ for } \ \text{w}<0 \end{cases} \tag{4}$$

In the space domain, the relationship between the input and output signals is expressed as a $g(r)$ composite function. $g(r)$ is an analytic function whose imaginary part is equal to the Hilbert transform of its real part.

$$g(r) = f(r) + jf_1(r), r = x + jz, \tag{5}$$

in which the Hilbert transform between the input and output signal in the space domain is defined as the mixture of the function in the input signal.

$$h(x) = F^{-1}(-j.\text{sgn}(w)), \tag{6}$$

$$h(x) = \frac{1}{\pi x}, \tag{7}$$

$$f_1(r) = h(x) * f(r), \tag{8}$$

$$f_1(r) = \frac{1}{\pi}\int_{-\infty}^{\infty} \frac{f(\theta)}{x-\theta} dv \tag{9}$$

Also, the phase angle can be achieved from (10) by the Hilbert transform.

$$z(t) = x(t) + jy(t) \tag{10}$$

where $z(t)$ is a function of time with instantaneous magnitude. The values of $a(t)$ and $\theta(t)$ can also be achieved using (11) and (12).

$$a(t) = \sqrt{x^2(t) + y^2(t)} \tag{11}$$

$$\theta(t) = \arctan\left(\frac{y(t)}{x(t)}\right) \tag{12}$$

Although the definition provided is the most conventional and basic definition for IF, there are also other definitions. The IF obtained using the analytical signal and the Hilbert conversion provides a meaningful physical concept of the signal, which is the phase angle change rate.

$$\omega(t) = \frac{d\theta}{dt} \tag{13}$$

Equation (14) is used to obtain IF after applying the Hilbert conversion to the input signal [27].

$$F = \frac{F_S}{2\pi} \times diff\left(angle\left(\bar{X}(t)\right)\right) \tag{14}$$

B. HIF detection algorithm

In the first stage, the algorithm samples the current signal and forms a signal window according to (15) [34].

$$\text{window length} = \frac{F_S}{F} \tag{15}$$

where F_S is the sampling frequency and is equal to 10 kHz and F is the base frequency of the power system which is considered to be 60 Hz. It should be noted that since the proposed algorithm can detect the faulty phase, the sampling and all the steps described below are separately executed in all three phases. In the next step, by obtaining samples from the main current signal, the effective value of available data will be calculated using (16) [35].

$$I_{rms} = \sqrt{\frac{\sum_{k=1}^{N} I_k^2}{N}} \quad (16)$$

Subsequently, according to the items mentioned in Section (II-A), IF is calculated along the signal window. After calculating the Hilbert transform and IF, a detection index (DI) should be calculated to detect the fault. Moving window averaging (MWA) is used to calculate the DI value. MWA is a low-pass filter applied to power system protection that is used for fault detection, fault direction detection, and faulty phase identification. This technique is less sensitive to noise in the signal. In MWA, the time domain of the continuous signal $x(t)$, for the T_0 length of the window is written as (17) [36].

$$\bar{x}(t) = \frac{1}{T_0} \int_{t-T_0}^{t} x(t)dt \quad (17)$$

The frequency response of the filter is the Fourier transform of the impulse response.

$$\bar{X}(j\omega) = e^{\frac{-j\omega T_0}{2}} \sin c\left(\frac{\omega T_0}{2}\right) \quad (18)$$

where $\sin c(\theta) = \sin(\theta)/\theta$.

Equation (19) indicates how to calculate DI.

$$\bar{X}(j\omega) = e^{\frac{-j\omega T_0}{2}} \sin c\left(\frac{\omega T_0}{2}\right) \quad (19)$$

The fault detection condition can be written based on (20).

$$DI > K \Rightarrow \text{HIF is detected} \quad (20)$$

where K is the threshold value obtained using various computer simulations. It is assumed to be 1.5 in this paper. The threshold value detection method used in this paper has already been discussed in references [3, 34].

With respect to the items expressed, the algorithm of the proposed method is provided in Fig. 1.

III. Simulation results

To simulate and test the method presented in different modes, the power system studied is simulated in Digsilent software. After analyzing the network in different cases, information is transferred from Digsilent software to MATLAB software to analyze and implement the proposed method. The protection algorithm presented in the previous section is implemented in the MATLAB m file and the desired outputs are received.

A. The network study

To test the proposed approach, an IEEE 39-bus system is implemented in this article. This network is a complex network with 10 synchronous generators. The specifications have made it very suitable for dynamic studies and the protection of power systems. Fig. 2 shows a single-line diagram of this network. The protection relay is installed on bus 26 to protect lines 29-26. The length of the protected line is 247.9688 km. This line is also parallel to lines 26-28 and 28-29. The length of the line, as well as the effects of the parallel lines, has made it very suitable for testing the proposed method.

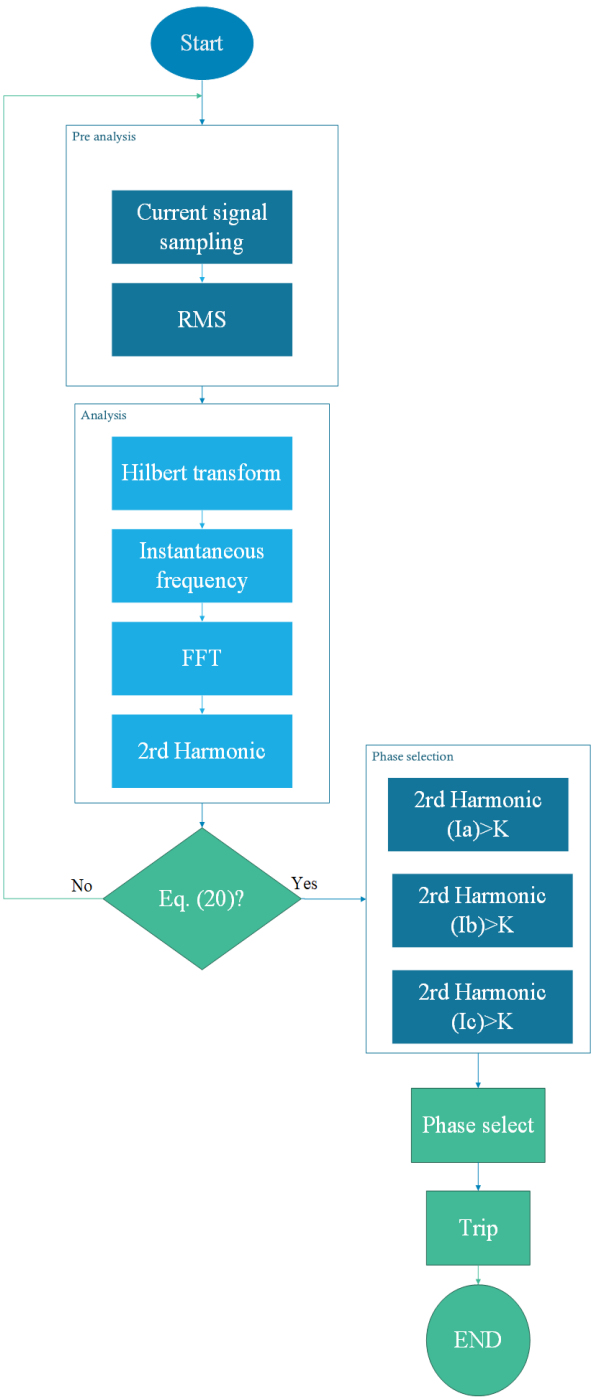

Fig. 1. The algorithm proposed for detecting HIF and determining the faulty phase.

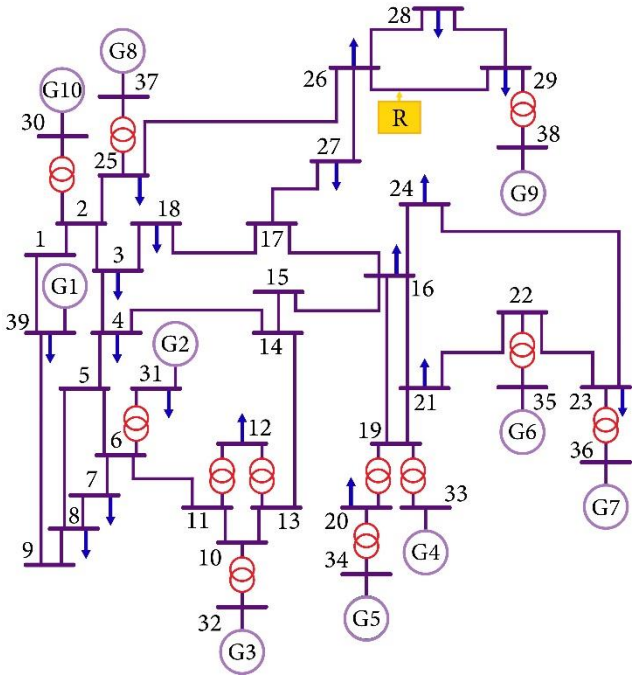

Fig. 2. The single-line diagram of the network.

B. *Case1: HIF detection*

Generally, power systems are exposed to various disturbances and anomalies that will highly affect their proper functioning. Among various faults, HIFs can be very challenging for power systems. During an HIF, the fault current is so limited; this amplitude can be very close to the capacitive bank switching current. Therefore, regular protection schemes cannot correctly detect this type of fault [37, 38]. For this reason, some other approaches are required to detect HIF and distinguish it from other regular power system events. The operation of the proposed method during HIF is described in this section and its performance during capacitive bank switching is presented in Section (III-D).

To evaluate the performance of the proposed method during a variety of HIFs, a single-phase HIF (the fault is applied to phase A) with R = 500 Ω and X = 50 Ω is first applied on 50% of the protected line. Fig. 3 shows the performance of the proposed method during this type of fault. According to this figure, after applying the fault, DI obtained in the final stage of the algorithm (Fig. 1) exceeded the threshold value, and the proposed algorithm sent the trip command within 9.72 ms. The algorithm also detected the faulty phase and sent the trip command only for phase A.

As mentioned earlier, HIF impedance may sometimes reach up to 1000 ohms. For this reason, an HIF with the same fault specifications and with the only difference that its fault impedance is 1000 ohms is implemented in the network. Fig. 4 shows the performance of the proposed algorithm during the HIF fault with R = 1000 Ω and X = 100 Ω. According to this figure, the algorithm could detect the fault in about 8 ms. The algorithm also detected the faulty phase, and the trip command was sent only to phase A.

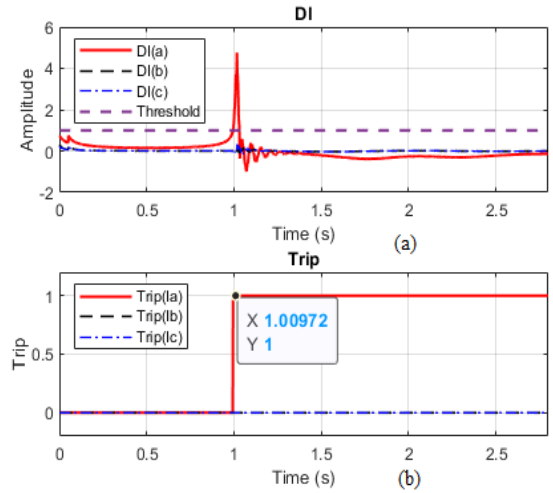

Fig. 3. Performance of the proposed method during a single-phase HIF fault with R = 500 Ω and X = 50 Ω, a) DI, b) Trip signal.

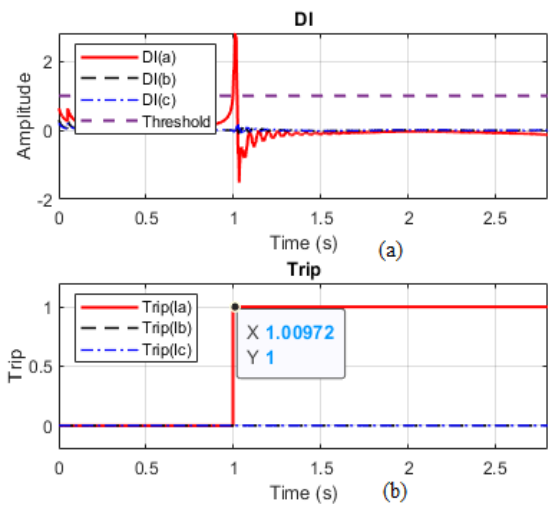

Fig. 4. Performance of the proposed method during a single-phase HIF with R = 1000 Ω and X = 100 Ω, a) DI, b) Trip signal.

As mentioned, the proposed algorithm can detect different HIF types. To validate this issue, a three-phase HIF with R = 500 Ω and X = 50 Ω was applied to the protected line in 1.5 s (Fig. 5). In another case, to investigate a fault with 1000 ohm impedance, a three-phase HIF with R = 1000 Ω and X = 100 Ω was applied to the protected line (Fig. 6). Evidently, the proposed method could detect the three-phase HIF. As can be seen, at this stage, the trip signal was sent to all three phases. According to Fig. 5, the trip command was sent within 11.9 ms, but in the three-phase HIF case with R = 1000 ohm and X = 100 ohms, the trip time was increased to 11.9 ms. Although the detection time of the algorithm was increased in this case, the detection time was still appropriate.

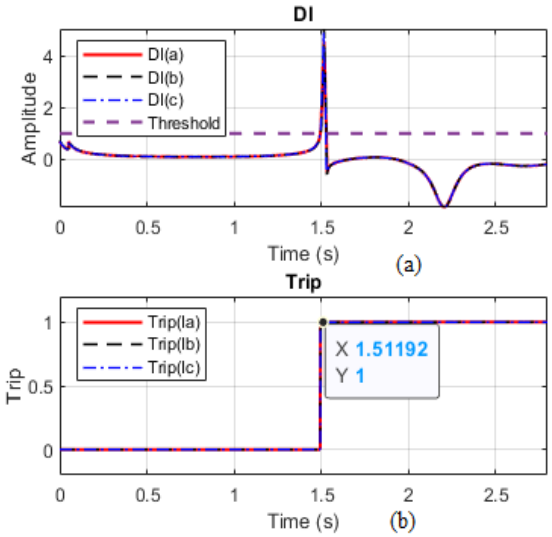

Fig. 5. Performance of the proposed method at the time of a three-phase HIF fault with R = 500 Ω and X = 50 Ω, a) DI, b) Trip signal.

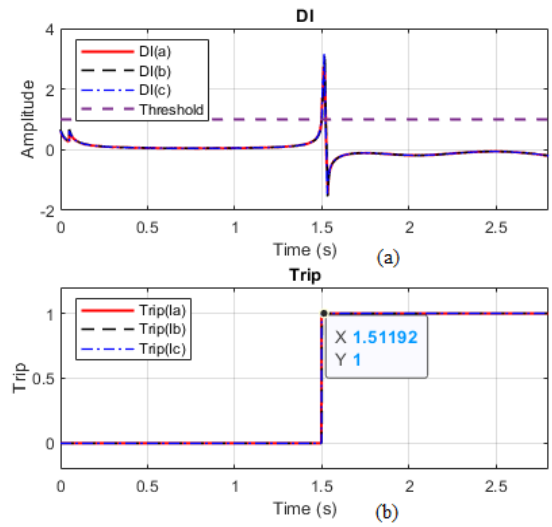

Fig. 6. Performance of the proposed method at the time of a three-phase HIF fault with R = 1000 Ω and X = 100 Ω, a) DI, b) Trip signal.

Figure 7 shows the performance of the proposed algorithm during various types of fault impedance angles. As it is clear from this figure, by changing the fault impedance angle, the performance of the proposed method has been appropriate.

A reverse fault current condition will occur when a fault occurs on one of the lines adjacent to the protected line. It should be mentioned that the presented method should only detect faults on the protected line and not other lines (detection of faults on adjacent lines may cause malfunction of the protection coordination, cascading outage of the transmission lines and even the network blackout). To further analyze this issue, a high impedance fault with R=500 Ω and X=50 Ω is placed on 50% of line 26-27. This causes the protection relay of line 26-29 to see a reverse current. Figure 8 shows the result of this test. As it is clear from this figure, since the fault is in the adjacent line, the relay did not operate. In fact, it can be said that the presented method works in a directional manner, which is considered as a positive feature for distance relays.

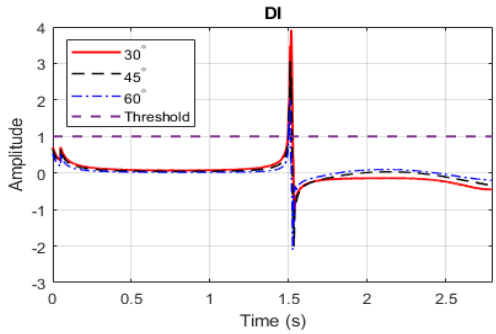

Fig. 7. The performance of the proposed method during different angles of fault impedance.

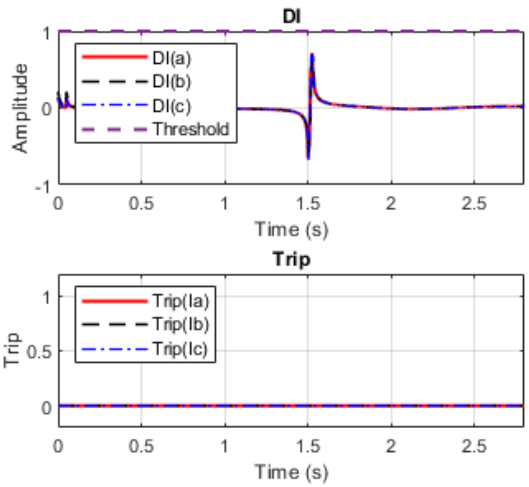

Fig. 8. Performance of the proposed method during a fault in adjacent lines

The impedance of a fault measured in the distance relay may become negative (i.e., a capacitator fault) in the compensated serial lines. Therefore, fault detection methods must be able to identify this type of fault, which was analyzed in this section. The fault was applied to 50% of the protected line at 1 s with different impedance angles. Figure 9 reports the test results. Accordingly, DI exceeded the threshold in all four cases, and the fault was detected correctly.

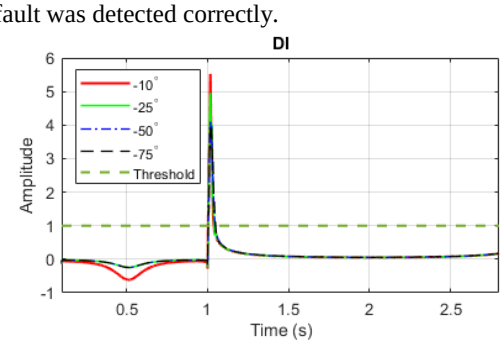

Fig. 9. The performance of the proposed method during different negative angles of fault impedance.

Fault angles can also affect the performance of HIF detection methods to some extent. For this reason, the effect of fault types and fault angles was also investigated. The results of this study are presented in Table 2. According to this table, the proposed method has a good performance for fault angles of 0, 30, and 90 degrees for different types of faults.

TABLE 2
PERFORMANCE OF THE PRESENTED METHOD IN DIFFERENT ANGLES OF HIF.

Fault type	Impedance	Fault angle	Detection time (ms)
A-G	R=100 Ω, X=10 Ω	0	9.7
	R=100 Ω, X=10 Ω	30	9.8
	R=100 Ω, X=10 Ω	90	9.7
B-G	R=200 Ω, X=20 Ω	0	9.7
	R=200 Ω, X=20 Ω	30	9.7
	R=200 Ω, X=20 Ω	90	9.9
C-G	R=300 Ω, X=30 Ω	0	9.7
	R=300 Ω, X=30 Ω	30	9.8
	R=300 Ω, X=30 Ω	90	9.7
A-B-G	R=400 Ω, X=40 Ω	0	11.9
	R=400 Ω, X=40 Ω	30	11.9
	R=400 Ω, X=40 Ω	90	11.9
A-C-G	R=500 Ω, X=50 Ω	0	11.7
	R=500 Ω, X=50 Ω	30	11.9
	R=500 Ω, X=50 Ω	90	11.9
B-C-G	R=1000 Ω, X=100 Ω	0	11.9
	R=1000 Ω, X=100 Ω	30	11.8
	R=1000 Ω, X=100 Ω	90	11.9
A-B-C	R=1000 Ω, X=100 Ω	0	11.9
	R=1000 Ω, X=100 Ω	30	11.8
	R=1000 Ω, X=100 Ω	90	11.9

C. *Case 2: LIF detection*

As was previously observed, the proposed algorithm can properly detect HIF. But to have a comprehensive protection algorithm, it should be able to detect low impedance fault (LIF) as well. To evaluate the performance of the proposed method in the LIF situation, a single-phase fault and a three-phase fault were applied to the protected line after 1.5 s. Figs. 10 and 11 illustrate the test results of the method provided during LIF faults. Obviously, the proposed algorithm correctly detected LIF. The only shortcoming of this algorithm is the lack of faulty phase detection and therefore the trip command was sent for all three phases (Fig. 10). Tackling this problem can be a suitable topic for further studies in this field.

As mentioned before, fault angle variations can significantly affect fault detection algorithms. Thus, the effects of different types of LIF and fault angles were also investigated. The results of this study are presented in Table 3 according to which the proposed method has a good performance for fault angles of 0, 30, and 90 degrees for different faults.

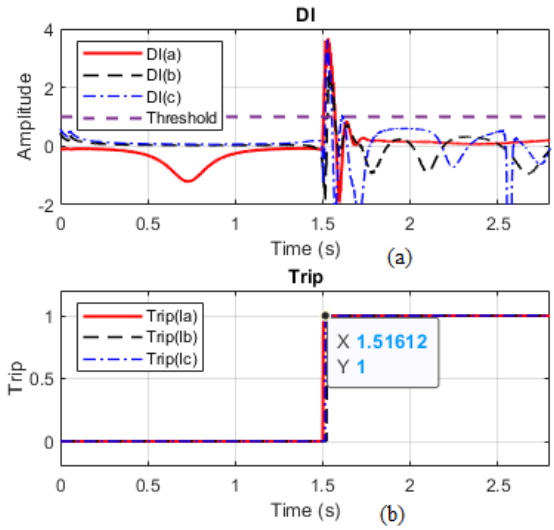

Fig. 10. Performance of the proposed method during a single-phase LIF, a) DI, b) Trip signal.

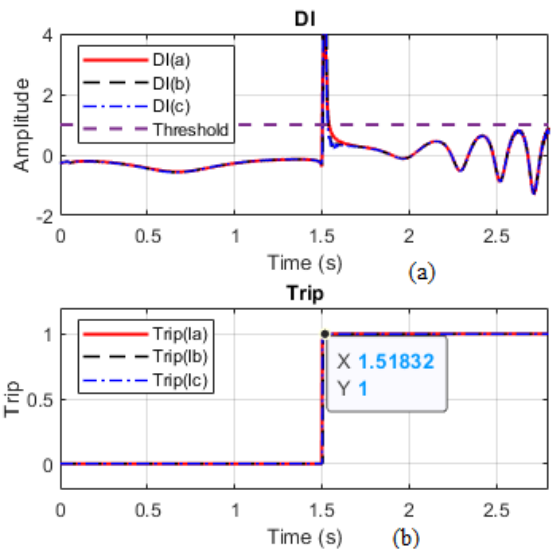

Fig. 11. Performance of the proposed method during a three-phase LIF, a) DI, b) Trip signal.

D. *Case 3: Capacitive bank switching*

As described earlier, current amplitude variations during HIF can be very similar to capacitive bank switching. For this reason, this section analyzes the performance of the proposed method during a capacitive bank switching. First, the performance of the proposed method during capacitive bank switching with RRP = 1 Mvar is investigated, and the results are illustrated in Fig. 12. The performance of the method during capacitive bank switching with RRP = 10 Mvar is also investigated and presented in Fig. 13. According to Figs. 12 and 10, during capacitive bank switching (1.5 seconds from the start of the simulation), the DI value has not exceeded the threshold value and the trip command is not issued. These two figures and the results obtained from previous tests prove that the proposed algorithm can appropriately distinguish between

capacitive bank switching, HIF, and LIF. Table 3 shows the performance of the presented method during all types of low-impedance faults. As it is clear from this table, the presented method has been able to quickly detect different types of low impedance faults.

TABLE 3
PERFORMANCE OF THE PRESENTED METHOD FOR DIFFERENT LIF ANGLES.

Fault type	Impedance	Fault angle	Detection time (ms)
A-G	R=0 Ω, X=0 Ω	0	16.1
	R=0 Ω, X=0 Ω	30	16.2
	R=0 Ω, X=0 Ω	90	16.1
B-G	R=0 Ω, X=0 Ω	0	16.1
	R=0 Ω, X=0 Ω	30	16.3
	R=0 Ω, X=0 Ω	90	16.1
C-G	R=0 Ω, X=0 Ω	0	16.2
	R=0 Ω, X=0 Ω	30	16.1
	R=0 Ω, X=0 Ω	90	16.1
A-B-G	R=0 Ω, X=0 Ω	0	18.2
	R=0 Ω, X=0 Ω	30	18.3
	R=0 Ω, X=0 Ω	90	18.4
A-C-G	R=0 Ω, X=0 Ω	0	18.3
	R=0 Ω, X=0 Ω	30	18.3
	R=0 Ω, X=0 Ω	90	18.1
B-C-G	R=0 Ω, X=0 Ω	0	18.3
	R=0 Ω, X=0 Ω	30	18.3
	R=0 Ω, X=0 Ω	90	18.3
A-B-C	R=0 Ω, X=0 Ω	0	18.2
	R=0 Ω, X=0 Ω	30	18.3
	R=0 Ω, X=0 Ω	90	18.3

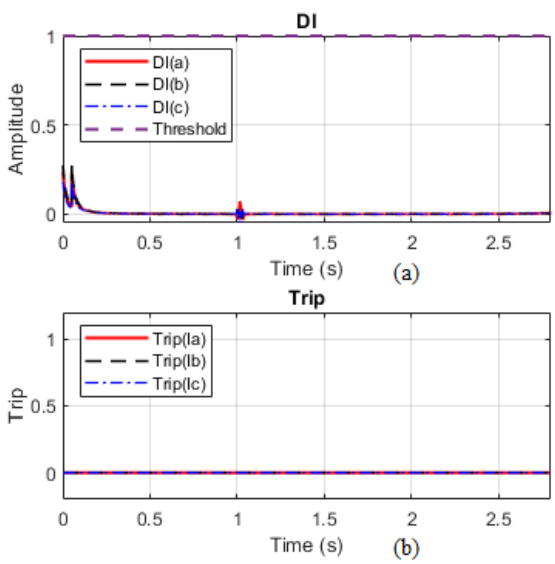

Fig. 12. Performance of the proposed method during capacitive bank switching with RRP = 1 MVar, a) DI, b) Trip signal.

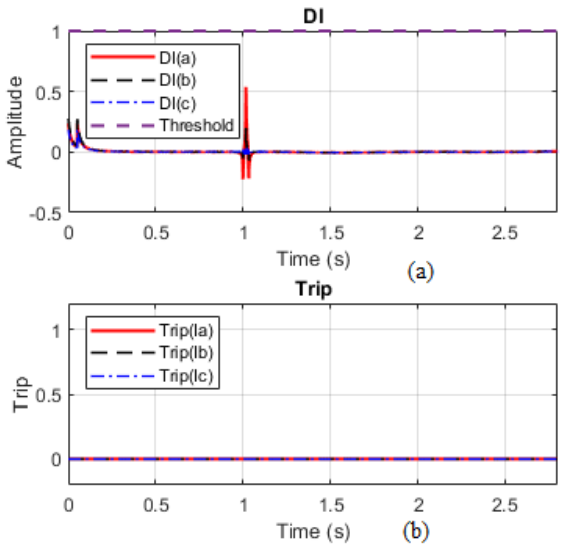

Fig. 13. Performance of the proposed method during capacitive bank switching with RRP = 10 MVar, a) DI, b) Trip signal.

E. Case 4: Noisy signal

In the real world, it is impossible to build a system without noise. Of course, it is possible to reduce the noise in the system by using solutions, but this noise will never reach zero. For this reason, it is best to design protection algorithms that are noise-resistant. White Gaussian noise is one of the types of noise that is widely used to investigate the effect of noise on protection algorithms [39]. White noise is generally referred to as a signal whose power is evenly distributed across all frequencies. White noise is inherently a Stochastic process. It is, therefore, a statistical model for signals and signal sources, not a specific signal. White Gaussian noise is any discrete signal at a time whose samples are a sequence of uncorrelated random variables with a mean of zero and finite variance. In this paper, white Gaussian noise with SNR = 10, 20, and 30 dB and Variance = 0.05 is used to test the proposed method. Figure 14 shows the performance of the method presented in different conditions when the signal is noisy. As it is clear from this figure, the proposed method has been able to detect different events simultaneously with noise.

F. Case 5: Wind turbine

To investigate the performance of the proposed method in a wind turbine case in an IEEE 39 bus network, two 500 and 400-MVA wind farms with a power factor of 0.8 are connected to bus 26 and two wind farms with similar specifications are connected to bus 29. The employed wind energy conversion system is a doubly-fed induction generator (DFIG). Subsequently, a three-phase fault with R=1000 Ω and X=100 Ω is placed in 50% of lines 26-29 in 1.5 seconds. Fig. 15 shows the test results of this fault in the network and in the presence of a wind turbine. As it is clear from this figure, the proposed method has been able to detect the high impedance fault in the presence of the wind turbine.

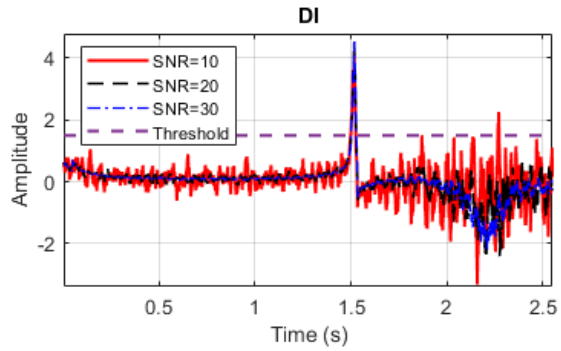

(a)

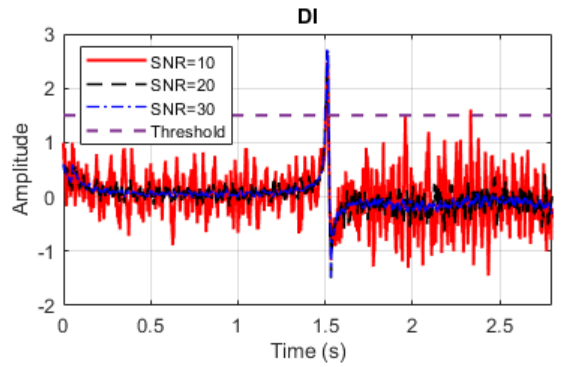

(b)

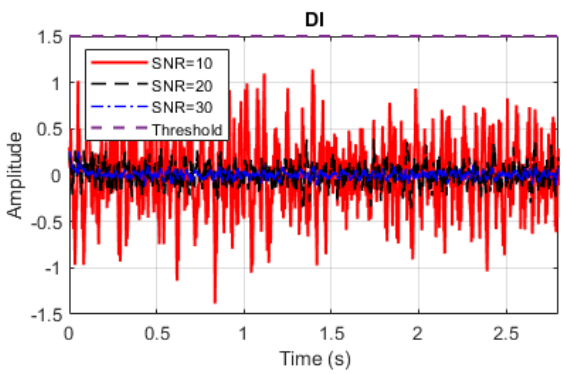

(c)

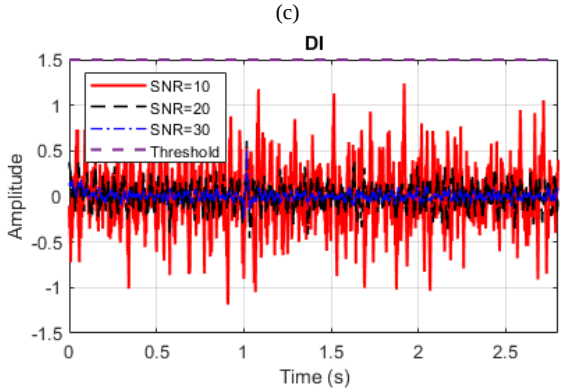

(d)

Fig. 14. Performance of the proposed method when the signal is noisy a) HIF with R = 500 Ω and X = 50 Ω b) HIF with R = 1000 Ω and X = 100 Ω c) capacitor bank switching with RRP = 1 Mvar d) capacitor bank switching with RRP = 10 Mvar.

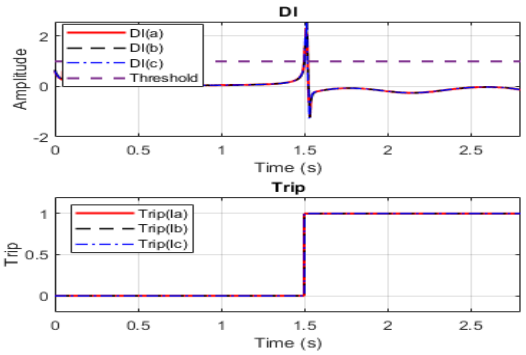

Fig. 15. The performance of the proposed method in the existence of a wind turbine in the studied network, a) DI, b) Trip signal.

G. Case 6: Two-area network

The single-line diagram of the two-area network is presented in Fig. 16. Accordingly, to protect line 1, the protection relay is connected to bus 7. To investigate the performance of this network during faults, a variety of HIFs are placed on 50% of line 1. The results of the HIF tests are presented in Table 4.

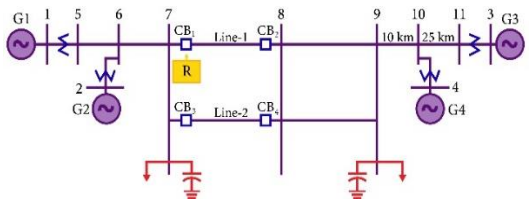

Fig. 16. The single-line diagram of the standard two-area network.

TABLE 4
PERFORMANCE OF THE PRESENTED METHOD IN DIFFERENT ANGLES OF HIF IN THE TWO-AREA NETWORK.

Fault type	Impedance	Fault angle	Detection time (ms)
A-G	R=100 Ω, X=10 Ω	0	9.8
	R=100 Ω, X=10 Ω	30	9.7
	R=100 Ω, X=10 Ω	90	9.8
B-G	R=200 Ω, X=20 Ω	0	9.7
	R=200 Ω, X=20 Ω	30	9.8
	R=200 Ω, X=20 Ω	90	9.7
C-G	R=300 Ω, X=30 Ω	0	9.7
	R=300 Ω, X=30 Ω	30	9.7
	R=300 Ω, X=30 Ω	90	9.8
A-B-G	R=400 Ω, X=40 Ω	0	12.1
	R=400 Ω, X=40 Ω	30	12.1
	R=400 Ω, X=40 Ω	90	12.2
A-C-G	R=500 Ω, X=50 Ω	0	12.1
	R=500 Ω, X=50 Ω	30	12.1
	R=500 Ω, X=50 Ω	90	122
B-C-G	R=1000 Ω, X=100 Ω	0	12.1
	R=1000 Ω, X=100 Ω	30	12.1
	R=1000 Ω, X=100 Ω	90	12.3
A-B-C	R=1000 Ω, X=100 Ω	0	12.1
	R=1000 Ω, X=100 Ω	30	12.3
	R=1000 Ω, X=100 Ω	90	12.1

IV. Conclusions

Faults are very likely to happen in power systems due to their accidental nature and environmental conditions. Therefore, power systems are in dire need of a proper protection system. A proper protection system with proper and timely operation can reduce damage to network equipment and even humans. Among the various protection designs and relays, distance relays are an integral part of the protection of power systems. These relays have desirable features such as simplicity, use of local voltage and current for fault detection, and fault locating capability. The distance relay features make it very suitable for protecting power transmission lines. But, despite the many advantages they provide, distance relays protection algorithms also have some shortcomings. For instance, they may malfunction during HIF.

For this reason, this paper presents a new method based on the Hilbert conversion and instantaneous frequency for HIF detection. The proposed method has been tested in an IEEE standard 39 bus network in different conditions of HIF, LIF, and capacitive bank switching. The results prove the applicability of the proposed method. Furthermore, the proposed method is resistant to white Gaussian noise and operates appropriately during signal noise.

REFERENCES

[1] J. Doria-Garcia, C. Orozco-Henao, L. Iurinic, and J. D. Pulgarín-Rivera, "High impedance fault location: Generalized exten-sion for ground faults," International Journal of Electrical Power & Energy Systems, vol. 114, p. 105387, 2020.

[2] J. Doria-García, C. Orozco-Henao, R. Leborgne, O. D. Montoya, and W. Gil-González, "High impedance fault modeling and location for transmission line," Electric Power Systems Research, vol. 196, p. 107202, 2021.

[3] B. Taheri, S. A. Hosseini, H. Askarian-Abyaneh, and F. Razavi, "Power swing detection and blocking of the third zone of distance relays by the combined use of empirical-mode decomposition and Hilbert transform," IET Generation, Transmission & Distribution, vol. 14, no. 6, pp. 1062-1076, 2019.

[4] S. Vlahinić, D. Franković, B. Juriša, and Z. Zbunjak, "Back up protection scheme for high impedance faults detection in transmission systems based on synchrophasor measurements," IEEE Transactions on Smart Grid, vol. 12, no. 2, pp. 1736-1746, 2020.

[5] B. Taheri and S. A. Hosseini, "Detection of High Impedance Fault in DC Microgrid Using Impedance Prediction Technique," in 2020 15th International Conference on Protection and Automation of Power Systems (IPAPS), 2020, pp. 68-73: IEEE.

[6] B. Taheri, S. A. Hosseini, S. Salehimehr, and F. Razavi, "A Novel Approach for Detection High Impedance Fault in DC Mi-crogrid," in 2019 International Power System Conference (PSC), 2020, pp. 287-292: IEEE.

[7] T. Lai, L. Snider, E. Lo, and D. Sutanto, "High-impedance fault detection using discrete wavelet transform and frequency range and RMS conversion," IEEE Transactions on Power Delivery, vol. 20, no. 1, pp. 397-407, 2005.

[8] S. Nezamzadeh-Ejieh and I. Sadeghkhani, "HIF detection in distribution networks based on Kullback–Leibler divergence," IET Generation, Transmission & Distribution, vol. 14, no. 1, pp. 29-36, 2020.

[9] R. Bhandia, J. de Jesus Chavez, M. Cvetković, and P. Palensky, "High impedance fault detection using advanced distortion detection technique," IEEE Transactions on Power Delivery, vol. 35, no. 6, pp. 2598-2611, 2020.

[10] W. Santos, F. Lopes, N. Brito, and B. Souza, "High-impedance fault identification on distribution networks," IEEE Transactions on Power Delivery, vol. 32, no. 1, pp. 23-32, 2016.

[11] M. S. Tonelli-Neto, J. G. M. Decanini, A. D. P. Lotufo, and C. R. Minussi, "Fuzzy based methodologies comparison for high-impedance fault diagnosis in radial distribution feeders," IET Generation, Transmission & Distribution, vol. 11, no. 6, pp. 1557-1565, 2017.

[12] I. Baqui, I. Zamora, J. Mazón, and G. Buigues, "High impedance fault detection methodology using wavelet transform and artificial neural networks," Electric Power Systems Research, vol. 81, no. 7, pp. 1325-1333, 2011.

[13] X. Wang et al., "High impedance fault detection method based on improved complete ensemble empirical mode decompo-sition for DC distribution network," International Journal of Electrical Power & Energy Systems, vol. 107, pp. 538-556, 2019.

[14] M. Faghihlou, B. Taheri, and S. Salehimehr, "High Impedance Fault Detection in DC Microgrid using Real and Imaginary Components of Power," in 2020 28th Iranian Conference on Electrical Engineering (ICEE), 2020.

[15] E. Sortomme, S. Venkata, and J. Mitra, "Microgrid protection using communication-assisted digital relays," IEEE Transac-tions on Power Delivery, vol. 25, no. 4, pp. 2789-2796, 2009.

[16] N. Faridnia, H. Samet, and B. D. Dezfuli, "A new approach to high impedance fault detection based on correlation func-tions," in IFIP International Conference on Artificial Intelligence Applications and Innovations, 2012, pp. 453-462: Springer.

[17] M. Kavi, Y. Mishra, and M. D. Vilathgamuwa, "High-impedance fault detection and classification in power system distribu-tion networks using morphological fault detector algorithm," IET Generation, Transmission & Distribution, vol. 12, no. 15, pp. 3699-3710, 2018.

[18] S. Gautam and S. M. Brahma, "Detection of high impedance fault in power distribution systems using mathematical mor-phology," IEEE Transactions on Power Systems, vol. 28, no. 2, pp. 1226-1234, 2012.

[19] H. Livani and C. Y. Evrenosoglu, "A machine learning and wavelet-based fault location method for hybrid transmission lines," IEEE Transactions on Smart Grid, vol. 5, no. 1, pp. 51-59, 2013.

[20] M. M. Ghalesefidi and N. Ghaffarzadeh, "A new phaselet-based method for detecting the power swing in order to prevent the malfunction of distance relays in transmission lines," Energy Systems, pp. 1-25, 2019.

[21] S. Salehimehr, B. Taheri, F. Razavi, M. Parpaei, and M. Faghihlou, "A new power swing detection method based on chaos theory," Electrical Engineering, pp. 1-19, 2019.

[22] B. Taheri and M. Sedighizadeh, "Detection of power swing and prevention of mal-operation of distance relay using com-pressed sensing theory," IET Generation, Transmission & Distribution, vol. 14, no. 23, pp. 5558-5570, 2020.

[23] R. F. Espinoza, O. Dias, M. C. Tavares, and Y. P. Molina, "Application of a robust faulted phase selector to high-

resistance and weak-infeed fault conditions on a 1000-kV UHV transmission line," Electric Power Systems Research, vol. 197, p. 107244, 2021.
[24] S. Roy and S. Debnath, "PSD based high impedance fault detection and classification in distribution system," Measure-ment, vol. 169, p. 108366, 2021.
[25] M. Paul and S. Debnath, "Wavelet based single Ended scheme for high impedance fault classification in transmission lines," in 2020 International Conference on Smart Technologies in Computing, Electrical and Electronics (ICSTCEE), 2020, pp. 157-162: IEEE.
[26] V. Ashok and A. Yadav, "Fault diagnosis scheme for cross-country faults in dual-circuit line with emphasis on high-impedance fault syndrome," IEEE Systems Journal, 2020.
[27] B. Taheri, S. Salehimehr, F. Razavi, and M. Parpaei, "Detection of power swing and fault occurring simultaneously with power swing using instantaneous frequency," Energy Systems, vol. 11, no. 2, pp. 491-514, 2020.
[28] H. Teimourzadeh, A. Moradzadeh, M. Shoaran, B. Mohammadi-Ivatloo, and R. Razzaghi, "High Impedance Single-Phase Faults Diagnosis in Transmission Lines via Deep Reinforcement Learning of Transfer Functions," IEEE Access, vol. 9, pp. 15796-15809, 2021.
[29] C. Rahmann and A. Castillo, "Fast frequency response capability of photovoltaic power plants: The necessity of new grid requirements and definitions," Energies, vol. 7, no. 10, pp. 6306-6322, 2014.
[30] A. Korpel, "Gabor: frequency, time, and memory," Applied optics, vol. 21, no. 20, pp. 3624-3632, 1982.
[31] S. Salehimehr, B. Taheri, S. A. Hosseini, H. Askarian Abyaneh, and F. Razavi, "A new power swing detection method based on hilbert transform," International Journal of Industrial Electronics, Control and Optimization, 2020.
[32] S. L. Hahn, Hilbert transforms in signal processing. Artech House Signal Processing, 1996.
[33] M. Feldman, "Hilbert transform in vibration analysis," Mechanical systems and signal processing, vol. 25, no. 3, pp. 735-802, 2011.
[34] S. Salehimehr, B. Taheri, and M. Faghihlou, "Detection of power swing and blocking the distance relay using the variance calculation of the current sampled data," Electrical Engineering, pp. 1-15, 2021.
[35] N. Kagan et al., "Influence of rms variation measurement protocols on electrical system performance indices for voltage sags and swells," in Ninth International Conference on Harmonics and Quality of Power. Proceedings (Cat. No. 00EX441), 2000, vol. 3, pp. 790-795: IEEE.
[36] Taheri, Behrooz, and Mostafa Sedighizadeh. "A moving window average method for internal fault detection of power transformers." Cleaner Engineering and Technology 4 (2021): 100195.
[37] R. B. Grimaldi, T. S. Chagas, J. Montalvao, N. S. Brito, W. C. dos Santos, and T. V. Ferreira, "High impedance fault detec-tion based on linear prediction," Electric Power Systems Research, vol. 190, p. 106846, 2021.
[38] J. C. García, V. V. García, and N. Kagan, "Detection of high impedance faults in overhead multi grounded networks," in 2014 11th IEEE/IAS International Conference on Industry Applications, 2014, pp. 1-6: IEEE.
[39] S. A. Hosseini, B. Taheri, H. A. Abyaneh, and F. Razavi, "Comprehensive power swing detection by current signal modeling and prediction using the GMDH method," Protection and Control of Modern Power Systems, vol. 6, no. 1, pp. 1-11, 2021.

Hassan Abniki is a power system engineer at the University of Tehran and Tavanir Co. His main research interests include power system protection, power system transient, and smart grid.

Mostafa Hajati Samsi power system engineer at the Qazvin Islamic Azad University and Vebko Co. His main research interests include power system protection.

Behrooz Taheri was born in Qazvin, Iran, in 1993. He received the B.S. degree in electrical power engineering in 2015. He is received his MSc degree in Electrical Engineering with high honors from Qazvin Islamic Azad University (QIAU), Qazvin, Iran, 2018. He is currently doing his Ph.D. at QIAU. First researcher among all university students in the Qazvin province in 2020, and 2022. He has also been a Member of young researchers and elite club since 2018. His research interests include Power system protection, Non-intrusive load monitoring, Microgrid, and Smart grid.

Seyed Amir Hosseini received his B.S. degree from Islamic Azad University of Najafabad, Isfahan, Iran, in 2008, M.S. degree from Tafresh University, Markazi, Iran, in 2011, and Ph.D. degree from Amirkabir University of Technology, Tehran, Iran, in 2017, all in electrical engineering. He was a Research Assistant for Niroo Research Institute (NRI), from 2014 to 2015. He is currently an Assistant Professor of Electrical and Computer Engineering Group, Golpayegan College of Engineering, Isfahan University of Technology, Golpayegan , Iran. His research interests include power system protection, power system analysis, and smart grids.

IECO

This page intentionally left blank.